

CLIMATE VARIABILITY

Nonlinear Aspects

M Ghil, University of California–Los Angeles, Los Angeles, CA, USA

Copyright 2003 Elsevier Science Ltd. All Rights Reserved.

Ghil, M

Département Terre-Atmosphère-Océan (TAO) and
Laboratoire de Météorologie Dynamique (LMD),
Ecole Normale Supérieure (ENS), Paris

Introduction

The global climate system is composed of a number of subsystems — atmosphere, biosphere, cryosphere, hydrosphere, and lithosphere — each of which has a distinct characteristic time, from days and weeks to centuries and millennia. Each subsystem, moreover, has its own internal variability, all other things being constant, over a fairly broad range of time scales. These ranges overlap between one subsystem and another. The interactions between the subsystems thus give rise to climate variability on all time scales.

We outline here the rudiments of the way in which dynamical systems theory is starting to provide an understanding of this vast range of variability. Such an understanding proceeds through the study of successively more complex flow patterns. These spatio-temporal patterns are studied within narrower ranges of time scales, such as intraseasonal, interannual, interdecadal and multimillennial; each of these frequency bands is covered in a separate article of this Encyclopedia. The main results of dynamical systems theory that are important for the study of climate involve essentially bifurcation theory and the ergodic theory of dynamical systems.

In the next section, we describe the climate system's dominant balance between incoming solar radiation and outgoing terrestrial radiation. This balance is consistent with the existence of multiple equilibria of surface temperatures. Such multiple equilibria are also present for other balances of climatic actions and reactions. Thus, on the intraseasonal time scale, the thermal driving of the mid-latitude westerly winds is countered by surface friction and mountain drag. Multiple equilibria typically arise from saddle-node bifurcations of the governing equations. Transitions from one equilibrium to another may result from small and random pushes, a typical case of minute causes having large effects in the long term.

In the following section, we sketch the ocean's overturning circulation between cold regions, where water is heavier and sinks, and warm regions, where it is lighter and rises. The effect of temperature on the density and, hence the motion, of the water masses is in competition with the effect of salinity: increases in density, through evaporation and brine formation, compete further with decreases in salinity and, hence, in density through precipitation and river runoff. These competing effects can also give rise to two distinct equilibria. In the present-day oceans, a thermohaline circulation prevails, in which the temperature effects dominate. In the remote past, about 50 My ago, a halothermal circulation may have obtained, with salinity effects dominating. In a simplified mathematical setting, these two equilibria arise by a pitchfork bifurcation that breaks the problem's mirror symmetry.

On shorter time scales, of decades to millennia, oscillations of intensity and spatial pattern in the thermohaline circulation seem to be the dominant mode of variability. We show how interdecadal oscillations in the ocean's circulation arise by Hopf bifurcation.

Energy-Balance Models and the Modeling Hierarchy

The methods of dynamical systems theory were applied first to simple models of atmospheric and oceanic flows, starting about 40 years ago. More powerful computers now allow their application to fairly realistic and detailed models of the atmosphere, the ocean, and the coupled atmosphere–ocean system. We start, therefore, by presenting such a hierarchy of models.

This presentation is interwoven with that of the successive bifurcations that lead from simple to more complex solution behavior for each climate model. Useful tools for comparing model behavior across the hierarchy and with observations are provided by ergodic theory. Among these, advanced methods for the analysis and prediction of univariate and multivariate time-series play an important role.

Radiation Balance and Energy-Balance Models (EBMs)

At present, the best-developed hierarchy is for atmospheric models. Atmospheric models were originally developed for weather simulation and prediction on

0110-P0020

0110-P0005

0110-P0010

0110-P0025

0110-P0015

0110-P0030

0110-P0035

0110-P0040

the time scale of hours to days. Currently they serve — in a stand-alone mode or coupled to oceanic and other models — to address climate variability on all time scales.

The first rung of the modeling hierarchy for the atmosphere is formed by zero-dimensional (0D) models; the number of model dimensions, from zero to three, refers to the number of independent space variables used to describe the model domain, that is to physical-space dimensions. Such 0D models essentially attempt to follow the evolution of global surface-air temperature \bar{T} as a result of changes in global radiative balance, as in eqns [1a, b, c].

$$c \frac{d\bar{T}}{dt} = R_i - R_o \quad [1a]$$

$$R_i = \mu Q_0 [1 - \alpha(\bar{T})] \quad [1b]$$

$$R_o = \sigma m(\bar{T}) \bar{T}^4 \quad [1c]$$

Here R_i and R_o are respectively incoming solar radiation and outgoing terrestrial radiation. The heat capacity c is that of the global atmosphere, plus that of the global ocean or some fraction thereof, depending on the time scale of interest: one might include in c only the ocean mixed layer when interested in subannual time scales but the entire ocean when studying paleoclimate. The rate of change of \bar{T} with time t is given by $d\bar{T}/dt$; Q_0 is the solar radiation received at the top of the atmosphere; σ is the Stefan–Boltzmann constant; and μ is an insolation parameter, equal to unity for present-day conditions. To have a closed, self-consistent model, the planetary reflectivity or albedo α and greyness factor m have to be expressed as functions of \bar{T} ; $m = 1$ for a perfectly black body and $0 < m < 1$ for a grey body like planet Earth.

There are two kinds of one-dimensional (1D) atmospheric models, for which the single spatial variable is latitude or height, respectively. The former are so-called energy-balance models (EBMs), which consider the generalization of the model [1] for the evolution of surface-air temperature $T = T(x, t)$, say, as in eqn [2].

$$c(x) \frac{\partial T}{\partial t} = R_i - R_o + D \quad [2]$$

Here the terms on the right-hand side can be functions of the meridional coordinate x (latitude, co-latitude, or sine of latitude), as well as of time t and temperature T . The horizontal heat flux term D expresses heat exchange between latitude belts; it typically contains

first and second partial derivatives of T with respect to x . Hence the rate of change of local temperature T with respect to time also becomes a partial derivative, $\partial T/\partial t$.

The first striking results of theoretical climate dynamics were obtained in showing that eqn [2] could have two stable steady-state solutions, depending on the value of the insolation parameter μ (see eqn [1b]). This multiplicity of stable steady states, or physically possible “climates” of our planet, can be explained, in its simplest form, in the 0D model [1]. The simple explanation resides in the fact that — for a fairly broad range of μ values around $\mu = 1.0$ — the curves for R_i and R_o as a function of \bar{T} intersect in three points. One of these corresponds to the present climate (highest \bar{T} value), and another to an ice-covered planet (lowest \bar{T} value); both of these are stable, while the third (intermediate \bar{T} values) is unstable. To obtain this result, it suffices to make two assumptions: (i) that $\alpha = \alpha(\bar{T})$ is a piecewise-linear function of \bar{T} , with high albedo at low temperature, due to the presence of snow and ice, and low albedo at high \bar{T} , due to their absence; and (ii) that $m = m(\bar{T})$ is a smooth, increasing function of \bar{T} that attempts to capture in its simplest form the “greenhouse effect” of trace gases and water vapor.

The bifurcation diagram of such a 1D EBM is shown in Figure 1. It displays the model’s mean temperature \bar{T} as a function of the fractional change μ in the insolation $Q = Q(x)$ at the top of the atmosphere. The S-shaped curve in the figure arises from two back-to-back saddle-node bifurcations. The normal form of the first one is given by eqn [3].

$$\dot{X} = \mu - X^2 \quad [3a]$$

Here X stands for a suitably normalized form of \bar{T} and $\dot{X} \equiv dX/dt$ is the rate of change of X , while μ is a parameter that measures the stress on the system, in particular a normalized form of the insolation parameter.

The uppermost branch corresponds to the steady-state solution $X = +\mu^{1/2}$ of eqn [3a] and is stable. It matches rather well the Earth’s present-day climate for $\mu = 1.0$; more precisely, the steady-state solution $T = T(x; \mu)$ of the full 1D EBM (not shown) matches closely the annual mean temperature profile from instrumental data over the last century.

The intermediate branch starts out at the left as the second solution, $X = -\mu^{1/2}$ of eqn [3a] and is unstable. It blends smoothly into the upper branch of a coordinate-shifted and mirror-reflected version of [3a], say as in eqn [3b].

$$\dot{X} = \mu - \mu_0 + (X - X_o)^2 \quad [3b]$$

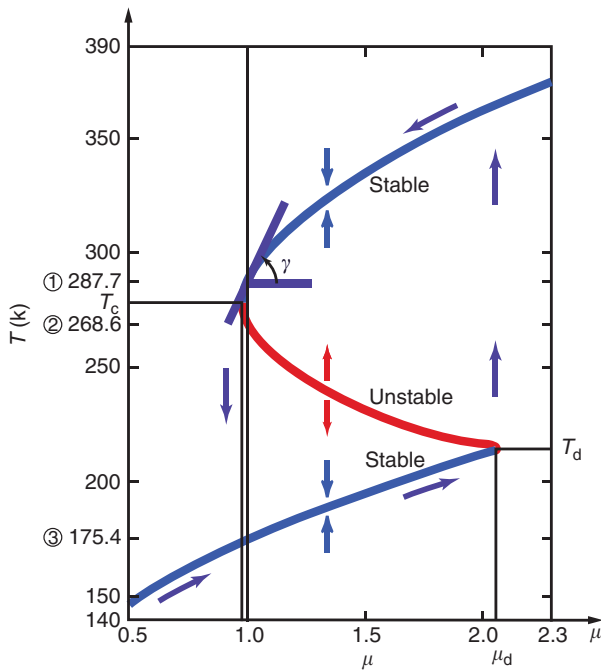


Figure 1 Bifurcation diagram for the solutions of an energy-balance model (EBM). Annual-mean temperature \bar{T} versus fractional change of insolation μ at the top of the atmosphere. The arrows pointing up and down at about $\mu = 1.4$ indicate the stability of the branches: towards a given branch if it is stable and away if it is unstable. The other arrows show the hysteresis cycle that global temperatures would have to undergo for transition from the upper stable branch to the lower one and back. The angle γ gives the measure of the present climate's sensitivity to changes in insolation. (After Ghil and Childress (1987).)

This branch, $X = X_0 + (\mu_0 - \mu)^{1/2}$, is also unstable. Finally, the lowermost branch in **Figure 1** is the second steady-state solution of eqn [3b], $X = X_0 - (\mu_0 - \mu)^{1/2}$, and is also stable. It corresponds to an ice-covered planet at the same distance from the Sun as is the Earth.

The fact that the upper-left bifurcation point in **Figure 1** is so close to present-day insolation values created great concern in the climate dynamics community in the mid-1970s, when these results were obtained. Indeed, much more detailed computations (see below) confirmed that a reduction of about 2–5% of insolation values would suffice to precipitate Earth into a “deep freeze.” The great distance of the lower-right bifurcation point from present-day insolation values, on the other hand, suggests that one would have to nearly double atmospheric opacity, say, for the Earth's climate to jump back to more comfortable temperatures.

Other Atmospheric Processes and Models

The 1D atmospheric models in which the details of radiative equilibrium are investigated with respect to a

height coordinate z (geometric height, pressure, etc.) are often called radiative-convective models. This name emphasizes the key role that convection plays in vertical heat transfer. While these models historically preceded EBMs as rungs on the modeling hierarchy, it was only recently shown that they, too, could exhibit multiple equilibria. The word (stable) “equilibrium,” here and in the rest of this article, refers simply to a (stable) steady state of the model, rather than a to true thermodynamic equilibrium.

Two-dimensional (2D) atmospheric models are also of two kinds, according to the third space coordinate, which is not explicitly included. Models that resolve explicitly two horizontal coordinates, on the sphere or on a plane tangent to it, tend to emphasize the study of the dynamics of large-scale atmospheric motions. They often have a single layer or two layers. Those that explicitly resolve a meridional coordinate and height are essentially combinations of EBMs and radiative-convective models and thereby emphasize the thermodynamic state of the system rather than its dynamics.

Yet another class of “horizontal” 2D models is the extension of EBMs to resolve zonal as well as meridional surface features, in particular land–sea contrasts. We will see below in discussing Bifurcation Diagrams for GCMs how such a 2-D EBM is used when coupled to an oceanic model.

Additional types of 1D and 2D atmospheric models are discussed and references to these and to the types discussed above are given by Schneider and Dickinson (1974) and by Ghil and Robertson (2000) (see Further Reading) along with some of their main applications. Finally, to encompass and resolve the main atmospheric phenomena with respect to all three spatial coordinates, general circulation models (GCMs) occupy the pinnacle of the modeling hierarchy.

The dependence of mean zonal temperature on the insolation parameter μ (the normalized “solar constant”) — as obtained for 1D EBMs and shown in **Figure 1** here — was confirmed, to the extent possible, by using a simplified GCM coupled to a “swamp” ocean model. More precisely, forward integrations with a GCM cannot confirm the presence of the intermediate, unstable branch. Nor was it possible in the mid-1970s, when this numerical experiment was done, to reach the “deep-freeze” stable branch, because of the computational limitations of the GCM. However, the parabolic shape of the upper branch (similar to the present day) near the upper-left bifurcation point in **Figure 1** (cf. eqn [3a]) was well supported by the GCM simulations.

Ghil and Robertson also describe the separate hierarchies that have grown over the last quarter-century in modeling the ocean and the coupled ocean–

atmosphere system. More recently, an overarching hierarchy of Earth-system models has been developing that encompasses all the subsystems of interest, atmosphere, biosphere, cryosphere, hydrosphere, and lithosphere. Eventually, the partial results about each subsystem's variability, outlined in this section and the next, will have to be verified from one rung to the next of the Earth-system modeling hierarchy.

Interdecadal Oscillations in the Thermohaline Circulation of the Oceans

Theory and Simple Models

Historically, the thermohaline circulation (THC) was first among the major process of the climate system to be studied using a very simple mathematical model. Stommel, in 1961 formulated a two-box model and showed that it possessed multiple equilibria.

A sketch of the Atlantic Ocean's THC and its interactions with the atmosphere and cryosphere on long time scales is shown in Figure 2. These interactions can lead to climate oscillations with multimillennial periods, such as the Heinrich events, and are summarized in the figure's caption. An equally schematic view of the global THC is provided by the widely known "conveyor belt" diagram; this diagram does not commonly include the interactions of the THC with water in both its gaseous and solid phases, which the former does include.

Basically, the THC is due to denser water sinking, lighter water rising, and water mass continuity closing the circuit through near-horizontal flow between the areas of rising and sinking. The effects of temperature and salinity on the density of the ocean water, $\rho = \rho(T, S)$, oppose each other: the density ρ decreases with increasing T and increases with increasing S . It is these two effects that give the thermohaline circulation its name, from the Greek words for heat and salinity. In high latitudes, ρ increases as the water loses heat to the air above and, if sea ice is formed, as the water underneath is enriched in brine. In low latitudes, ρ increases owing to evaporation but decreases owing to sensible heat flux into the ocean.

For the present climate, the temperature effect is stronger than the salinity effect, and ocean water is observed to sink in certain areas of the high-latitude North Atlantic and Southern Ocean — with very few and limited areas of deep-water formation elsewhere — and to rise everywhere else. Thus in thermohaline circulation, T is more important than and hence comes before S . During some remote geological times, deep water may have formed in the global ocean near the Equator; such an overturning circulation of opposite sign to that prevailing today has been dubbed halothermal (S before T). The quantification of the relative effects of T and S on the buoyancy of the oceanic water masses in high and low latitudes is far from complete, especially for paleocirculations; the association of the latter with salinity effects that exceed the thermal ones is thus rather tentative.

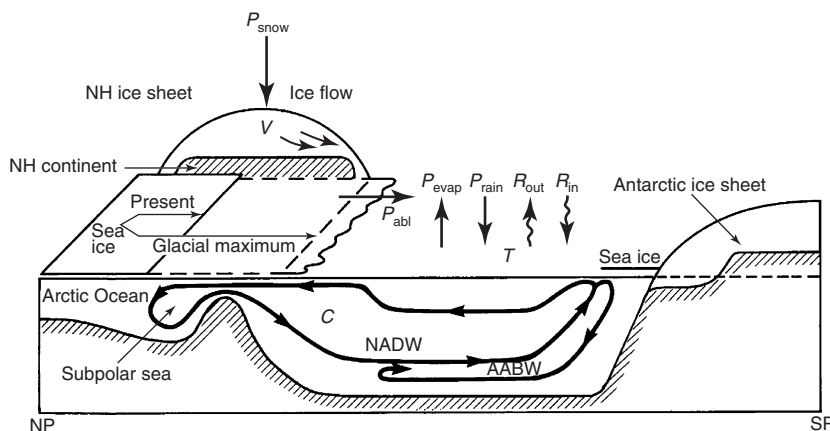


Figure 2 Diagram of an Atlantic meridional cross-section from North Pole (NP) to South Pole (SP), showing mechanisms likely to affect the thermohaline circulation (THC) on various time scales. Changes in the radiation balance $R_{in} - R_{out}$ are due, at least in part, to changes in extent of Northern Hemisphere (NH) snow and ice cover, V , and how they affect the global temperature, T ; the extent of Southern Hemisphere ice is assumed constant, to a first approximation. The change in hydrological cycle expressed in the terms $P_{rain} - P_{evap}$ for the ocean and $P_{snow} - P_{abl}$ for the snow and ice is due to changes in ocean temperature. Deep-water formation in the North Atlantic Subpolar Sea (North Atlantic Deep Water: NADW) is affected by changes in ice volume and extent, and regulates the intensity C of the THC; changes in Antarctic Bottom Water (AABW) formation are neglected in this approximation. This in turn affects the system's temperature, and is also affected by it. (After Ghil *et al.* (1987).)

0110-P0130 Stommel considered a two-box model, with two pipes connecting the two boxes. He showed that the system of two nonlinear, coupled ordinary differential equations that govern the temperature and salinity differences between the two well-mixed boxes has two stable steady-state solutions, distinguished by the direction of flow in the upper and lower pipes. Stommel's paper was primarily concerned with distinct local convection regimes, and hence vertical stratifications, in the North Atlantic and Mediterranean (or Red Sea), say. Today, we mainly think of one box as representing the low latitudes and the other as representing the high latitudes in the global THC.

0110-P0135 The next step in the hierarchical modeling of the THC is that of 2D meridional plane models, in which the temperature and salinity fields are governed by coupled nonlinear partial differential equations with two independent space variables: latitude and depth, say. Given boundary conditions for such a model that are symmetric about the Equator, as are the equations themselves, one expects a symmetric solution, in which water either sinks near the poles and rises everywhere else (thermohaline) or sinks near the Equator and rises everywhere else (halothermal). These two symmetric solutions would correspond to the two equilibria of Stommel's box model of 1961.

0110-P0140 In fact, symmetry breaking can occur, leading gradually from a symmetric two-cell circulation to an antisymmetric one-cell circulation. In between, all degrees of dominance of one cell over the other are possible. A situation lying somewhere between the two seems to resemble most closely the meridional overturning diagram of the Atlantic Ocean in Figure 2.

0110-P0145 This symmetry breaking can be described by a pitchfork bifurcation:

$$\dot{X} = \mu X - X^3 \quad [4]$$

Here X stands for the amount of asymmetry in the solution, so that $X = 0$ is the symmetric branch, and μ is a parameter that measures the stress on the system, in particular a normalized form of the buoyancy flux at the surface. For $\mu < 0$, the symmetric branch is stable;

for $\mu > 0$, the two branches $X = \pm\mu^{1/2}$ inherit its stability.

0110-P0150 In the 2D THC problem, the left cell dominates on one branch, while the right cell dominates on the other: for a given value of μ , the two stable steady-state solutions — on the $\{X = +\mu^{1/2}\}$ branch and on the $\{X = -\mu^{1/2}\}$ branch — are mirror images of each other. The idealized THC in Figure 2, with the North Atlantic Deep Water extending to the Southern Ocean's polar front, corresponds to one of these two branches. In theory, therefore, a mirror-image circulation, with the Antarctic Bottom Water extending to the North Atlantic's polar front, is equally possible.

Bifurcation Diagrams for GCMs

0110-P0155 Bryan was the first, in 1986, to document transition from a two-cell to a one-cell circulation in a simplified ocean GCM with idealized, symmetric forcing. Results of coupled ocean-atmosphere GCMs, however, have led to questions about the realism of more than one stable THC equilibrium. The situation with respect to the THC's pitchfork bifurcation (eqn [4]) is thus subtler than it was with respect to Figure 1 for radiative equilibrium. While in the previous section atmospheric GCMs confirmed essentially the EBM results, the results obtained in climbing the rungs of the modeling hierarchy for the THC are still in need of further clarification.

0110-P0160 Internal variability of the THC — with smaller and more regular excursions than the huge and irregular jumps associated with bistability — was studied intensively in the late 1980s and the 1990s. These studies placed themselves on various rungs of the modeling hierarchy, from box models through 2D models, and all the way to ocean GCMs. A summary of the different kinds of oscillatory variability found in the latter appears in Table 1. Such oscillatory behavior seems to match more closely the instrumentally recorded THC variability, as well as the paleoclimatic records for the recent geological past, than does bistability.

0110-P0165 The (multi)millennial oscillations interact with variability in the surface features and processes shown

0110-T0001 **Table 1** Thermohaline circulation (THC) oscillations

<i>Time scale</i>	<i>Phenomenon</i>	<i>Mechanism</i>
Interdecadal	3D, wind-driven+thermohaline circulation	Gyre advection
Centennial	Loop-type, Atlantic–Pacific circulation	Localized surface-density anomalies due to surface coupling
Millennial	Relaxation oscillation, with “flushes” and superimposed decadal fluctuations	Conveyor-belt advection of high-latitude density anomalies Bottom-water warming, due to high-latitude freshening and its braking effect

Adapted from Ghil (1994).

in Figure 2. Chen and Ghil, in particular, studied some of the interactions between atmospheric processes and the THC. They used a so-called hybrid coupled model, namely, a (horizontally) 2D EBM coupled to a rectangular-box version of the North Atlantic rendered by a low-resolution ocean GCM. This hybrid model's regime diagram is shown in Figure 3A. A steady state is stable for high values of the coupling parameter λ_{ao} or of the EBM's diffusion parameter d . Interdecadal oscillations with a period of 40–50 years are self-sustained and stable for low values of these parameters.

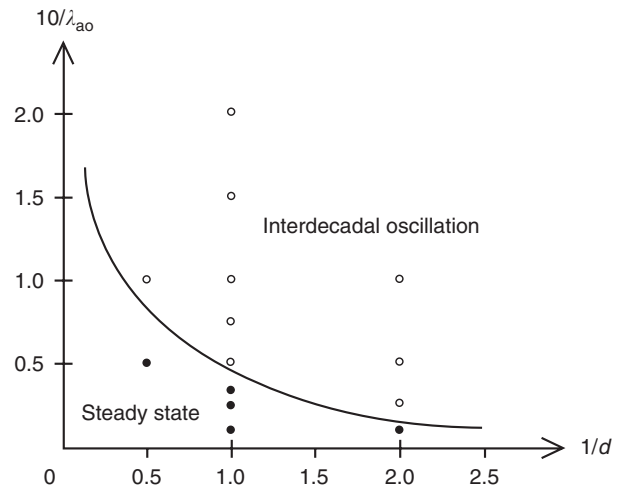
The self-sustained THC oscillations in question are characterized by a pair of vortices of opposite sign that grow and decay in quadrature with each other in the ocean's upper layers. Their centers follow each other anticlockwise through the north-western quadrant of the model's rectangular domain. Both the period and the spatiotemporal characteristics of the oscillation are thus rather similar to those seen in a fully coupled GCM with realistic geometry. The transition from a stable equilibrium to a stable limit cycle, via Hopf bifurcation, in this hybrid coupled model, is shown in Figure 3B.

Concluding Remarks

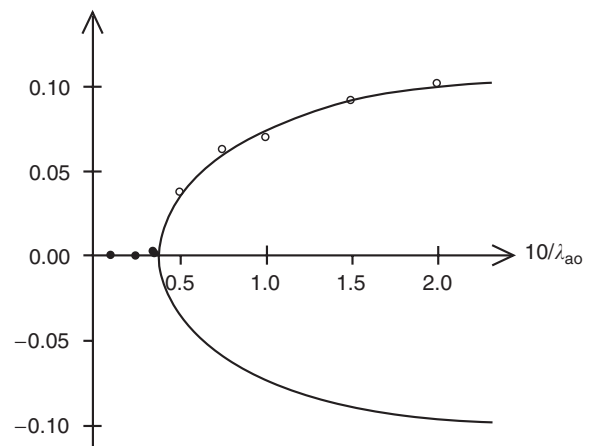
A complete theory of climate variability, across the entire range of time scales of interest, is still in the future. We have shown, though, that powerful conceptual and numerical tools exist to organize the emerging knowledge so far. The approach described herein has progressed from its first modest steps — taken to understand very simple models, almost half a century ago — to the analysis of the behavior of atmospheric, oceanic, and coupled GCMs. It is quite possible that equally large strides forward will be taken over the lifespan of this Encyclopedia.

See also

Climate Variability: Decadal to Centennial Variability (0107); Glacial, Interglacial Variations (0108); Seasonal to Interannual Variability (0029). **Global Change:** Biospheric Impacts and Feedbacks (0472); Human Impact of Climate Change (0001); Ozone Trends (0002); Surface Temperature Trends (0005); Upper Atmospheric Change (0007). **Ocean Circulation:** General Processes (0276); Surface-Wind Driven Circulation (0280); Thermohaline Circulation (0281); Water Types and Water Masses (0279). **Paleoclimatology:** Ice Cores (0304); Varves (0305). **Weather Regimes and Multiple Equilibria** (0465).



(A)



(B)

Figure 3 Dependence of THC solutions on two parameters in a hybrid coupled model; the two parameters are the atmosphere–ocean thermal coupling coefficient λ_{ao} and the atmospheric thermal diffusion coefficient d . (A) Schematic regime diagram. The solid circles stand for the model's stable steady states, the open circles for stable limit cycles, and the curve is the estimated neutral stability curve between the former and the latter. (B) Hopf bifurcation curve at fixed $d = 1.0$ and varying λ_{ao} ; this curve was obtained by fitting a parabola to the model's numerical-simulation results, shown as solid and open circles. (From Chen and Ghil (1996).)

Further Reading

- Bryan F (1986) High-latitude salinity effects and interhemispheric thermohaline circulations. *Nature* 323: 301–304.
- Chen F and Ghil M (1996) Interdecadal variability in a hybrid coupled ocean–atmosphere model. *Journal of Physical Oceanography* 26: 1561–1578.
- Dijkstra HA (2000) *Nonlinear Physical Oceanography: A Dynamical Systems Approach to the Large-Scale Ocean Circulation and El Niño*. Dordrecht/Norwell, MA: Kluwer Academic.

- Eckmann J-P and Ruelle D (1985) Ergodic theory of chaos and strange attractors. *Reviews of Modern Physics* 57: 617–656 (addendum 57: 1115).
- Ghil M (1994) Cryothermodynamics: the chaotic dynamics of paleoclimate. *Physica D* 77: 130–159.
- Ghil M and Childress S (1987) *Topics in Geophysical Fluid Dynamics: Atmospheric Dynamics, Dynamo Theory and Climate Dynamics*. New York: Springer-Verlag.
- Ghil M and Robertson AW (2000) Solving problems with GCMs: General circulation models and their role in the climate modeling hierarchy. In: Randall D (ed.) *General Circulation Model Development: Past, Present and Future*, pp. 285–325. San Diego: Academic Press.
- Ghil M, Mullhaupt A and Pestiaux P (1987) Deep water formation and Quaternary glaciations. *Climate Dynamics* 2: 1–10.
- Ghil M, Allen MR, Dettinger MD, *et al.* (2002) Advanced spectral methods for climatic time series. *Reviews of Geophysics* (in press).
- Guckenheimer J and Holmes P (1983) *Nonlinear Oscillations, Dynamical Systems and Bifurcations of Vector Fields*. New York: Springer-Verlag.
- Kennett RP and Stott LD (1991) Abrupt deep-sea warming, paleoceanographic changes and benthic extinctions at the end of the Palaeocene. *Nature* 353: 225–229.
- Marotzke J (2000) Abrupt climate change and thermohaline circulation: mechanisms and predictability. *Proceedings of the National Academy of Sciences of the USA* 97: 1347–1350.
- North GR, Cahalan RF and Coakley JA Jr (1981) Energy balance climate models. *Reviews of Geophysics and Space Physics* 19: 91–121.
- Ramanathan V and Coakley JA (1978) Climate modeling through radiative convective models. *Reviews of Geophysics and Space Physics* 16: 465–489.
- Schneider SH and Dickinson RE (1974) Climate modeling. *Reviews of Geophysics and Space Physics* 25: 447–493.
- Stommel H (1961) Thermohaline convection with two stable regimes of flow. *Tellus* 13: 224–230.